

# Diiron(III) and polymeric iron(III)–sodium complexes with bridging and terminal pyridonate ligands: structures and magnetic properties †

Alexander J. Blake, Craig M. Grant, Simon Parsons, Gregory A. Solan and Richard E. P. Winpenny\*

Department of Chemistry, The University of Edinburgh, West Mains Road, Edinburgh EH9 3JJ, UK

The reaction of anhydrous iron(III) chloride or  $[\text{NEt}_4]_2[\text{Fe}_2\text{Cl}_6\text{O}]$  with equimolar quantities of 6-chloro-2-pyridone (Hchp) and NaOMe in MeOH afforded, after recrystallisation from tetrahydrofuran (thf), the one-dimensional polymer  $[\{\text{Fe}(\mu\text{-chp})_6\text{Na}_3(\mu\text{-MeOH})_6\cdot 2\text{thf}\}_n]$  **1**. When the reaction of  $\text{FeCl}_3$  with NaOMe and Hchp was performed in the presence of 4,4'-dimethyl-2,2'-bipyridine (dmbipy) or 1,10-phenanthroline (phen) the dinuclear complexes  $[\text{Fe}_2(\mu\text{-OMe})_2(\text{chp})_4(\text{dmbipy})_2]\cdot 2\text{MeOH}$  **2** or  $[\text{Fe}_2(\mu\text{-OMe})_2(\text{chp})_4(\text{phen})_2]\cdot 2\text{MeOH}$  **3** resulted. The molecular structures at 150 K and magnetic properties between 1.8 and 280 K of **1–3** have been investigated. Complex **1** displays magnetic behaviour consistent with a paramagnet while **2** and **3** exhibit antiferromagnetic exchange interactions between the spins of the iron(III) ions through OMe bridges ( $J = -26.8$  to  $-28.6$   $\text{cm}^{-1}$ ).

Complexes containing the Fe–O–Fe or Fe–O(R)–Fe (R = H or alkyl) units continue to be of considerable interest as a result of their relevance to biological systems and interesting magnetic properties.<sup>1</sup> Two iron(III) centres undergo antiferromagnetic exchange interactions through the oxygen bridge, the strength of which is dependent on the precise nature of the bridge, the exchange for  $\mu$ -oxo complexes ( $-J = 80\text{--}120$   $\text{cm}^{-1}$ ) being stronger than for  $\mu$ -hydroxo/ $\mu$ -alkoxo complexes ( $J = 1.2$  to  $-25$   $\text{cm}^{-1}$ ).<sup>1,2</sup>

Much effort has been made to generate Fe–O–Fe complexes with carboxylates as co-bridging ligands to model the haemerythrin diiron site.<sup>3</sup> In the same way Fe–O(R)–Fe (R = H or alkyl) carboxylate complexes have been the subject of several reports.<sup>4</sup> It has been shown by our group and others that the anion of 2-pyridone (2-hydroxypyridine) and its derivatives can behave as 1,3-bridging ligands *via* the ring nitrogen and the exocyclic oxygen atom in transition-metal complexes in a manner similar to carboxylates.<sup>5</sup> In this paper we investigate the chemistry of one member of the pyridone family of ligands, 6-chloro-2-pyridone (Hchp) and the reactions of its anion (chp) with anhydrous iron(III) chloride and with the  $\mu$ -O complex  $[\text{NEt}_4]_2[\text{Fe}_2\text{Cl}_6\text{O}]$ . The effect of the presence of the bidentate ligands 4,4'-dimethyl-2,2'-bipyridine (dmbipy) and 1,10-phenanthroline (phen), has been examined and three new complexes characterised (Scheme 1). In addition, the magnetic behaviour of all the new complexes has been studied. A portion of this work has been the subject of a preliminary report.<sup>6</sup>

## Results and Discussion

### (a) Syntheses and characterisation of complexes 1–3

Complex **1** was synthesised from the reaction of anhydrous  $\text{FeCl}_3$  or  $[\text{NEt}_4]_2[\text{Fe}_2\text{Cl}_6\text{O}]$ <sup>7</sup> with equimolar amounts of sodium methoxide and Hchp in MeOH and recrystallised from tetrahydrofuran (thf). Structure determination at 150 K revealed a one-dimensional heterobimetallic polymer of stoichiometry  $[\{\text{Fe}(\text{chp})_6\text{Na}_3(\text{MeOH})_6\cdot 2\text{thf}\}_n]$  **1**, a portion of which is shown in Fig. 1. Selected bond distances and angles are listed in Table 1.

The crystal structure of complex **1** reveals a crystallographic three-fold axis coincident with the metallic 'backbone' of the

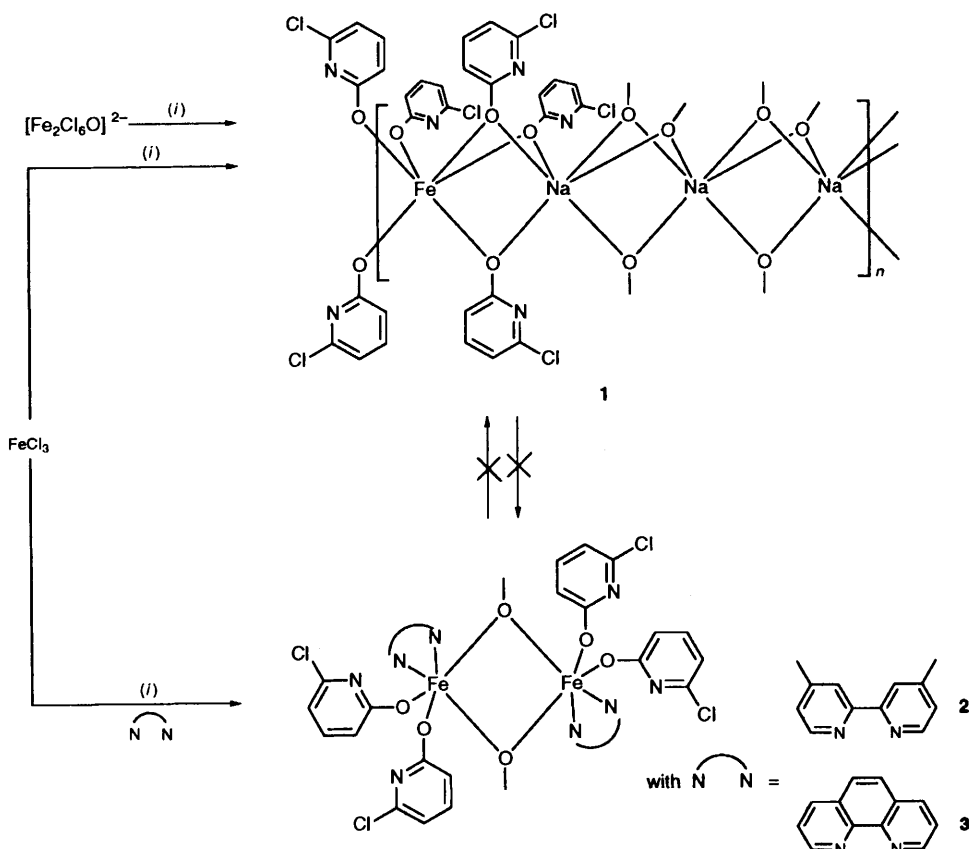
polymer. The atom Fe(1) is on a crystallographic  $\bar{3}$  axis, *i.e.* an  $S_6$  site, and is bound to six symmetry-equivalent oxygen atom donors from chp ligands. Three of these chp oxygen atoms bridge to Na(2), which lies on the three-fold axis, and three to a symmetry-equivalent sodium. Atom Na(2) is additionally bound to three methanol ligands, which are shared with Na(1). As Na(1) also lies on a  $\bar{3}$  site its co-ordination sphere is completed by three further methanol ligands, which in turn bridge to a further sodium, which is symmetry equivalent to Na(2). Thus all chp and methanol ligands within the structure act as bridging ligands through oxygen donor atoms. In our preliminary report on the structure of **1** the quality of the X-ray data (recorded at 293 K) led to some doubt as to whether the polymeric chain should be formulated as  $[\{\text{Fe}(\text{chp})_6\text{Na}_3(\text{MeOH})_6\}_n]$  or  $[\{\text{Fe}(\text{Hchp})_6\text{Na}_3(\text{OMe})_6\}_n]$ .<sup>6</sup> The improved quality of the crystals coupled with data collection at 150 K have now allowed the location of the MeOH hydrogen atom which forms a hydrogen bond to the chp nitrogen atom [H–OMe 0.982(3), N...HOMe 1.856(3) Å].

There are thus three distinct metal sites within the structure of complex **1**. The iron site involves six oxygen atoms arranged in a regular octahedral array, with Fe–O bond lengths of 1.999(2) Å. Atom Na(1) is also octahedrally co-ordinated, with the largest deviation from regularity being an angle of 83.6(1)°. Atom Na(2) has a much more distorted co-ordination geometry, with angles between the three chp O-atoms of 70.0(1)°. The Na–O bonds within the polymer are very slightly dependent on the source of the O atom; bonds to MeOH oxygens are between 2.383(2) and 2.369(2) Å, while those involving chp oxygens are 2.342(2) Å. Of the two metal–metal contacts within the polymer, Fe...Na(2) 3.017(2) Å is marginally shorter than Na(1)...Na(2) 3.047(2) Å.

Within the crystal of complex **1** the polymeric chains are arranged with the shortest potential interpolymer interaction occurring between a pyridone H atom and the centroid of a pyridone ring in a neighbouring polymer (H...centroid 2.94 Å) (Fig. 2). Disordered molecules of thf lie in the channels created by the  $[\{\text{Fe}(\text{chp})_6\text{Na}_3(\text{MeOH})_6\}_n]$  chains, without forming any significant contacts (not shown in Fig. 2).

Addition of the bidentate ligands dmbipy or phen to equimolar quantities of sodium methoxide and Hchp in a methanol solution of anhydrous iron(III) chloride resulted in the centrosymmetric dimeric complexes  $[\text{Fe}_2(\mu\text{-OMe})_2(\text{chp})_4(\text{dmbipy})_2]\cdot 2\text{MeOH}$  **2** and  $[\text{Fe}_2(\mu\text{-OMe})_2(\text{chp})_4(\text{phen})_2]\cdot 2\text{MeOH}$  **3** respectively. Crystals of **2** and **3** suitable for single

† Non-SI unit employed:  $\mu_B \approx 9.27 \times 10^{-24}$  J T<sup>-1</sup>.



**Scheme 1** Products from the reactions of the iron(III) chlorides  $\text{FeCl}_3$  and  $[\text{NET}_4]_2[\text{Fe}_2\text{Cl}_6\text{O}]$  with  $\text{Na}(\text{chp})$ . (i)  $\text{NaOMe}$ ,  $\text{Hchp}$ ,  $\text{MeOH}$

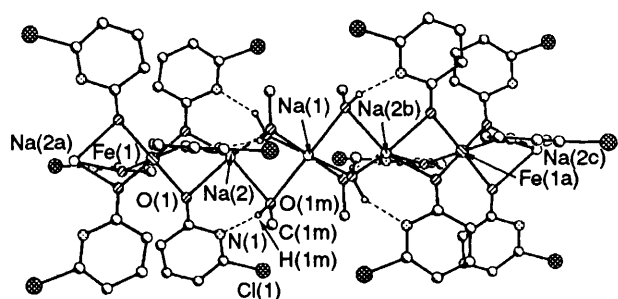


**Fig. 1** Molecular structure of complex **1** including the atom numbering scheme

**Table 1** Selected bond distances (Å) and angles (°) for complex **1**

$\text{Fe}(1)\text{--O}(1)$	1.999(2)	$\text{Fe}(1)\cdots\text{Na}(2)$	3.017(2)
$\text{Na}(1)\text{--O}(1\text{m})$	2.369(2)	$\text{Na}(1)\cdots\text{Na}(2)$	3.047(2)
$\text{Na}(2)\text{--O}(1)$	2.342(2)	$\text{N}(1)\cdots\text{H}(1\text{m})$	1.856(3)
$\text{Na}(2)\text{--O}(1\text{m})$	2.383(2)		
$\text{O}(1)\text{--Fe}(1)\text{--O}(1\text{a})$	95.6(1)	$\text{O}(1)\text{--Na}(2)\text{--O}(1\text{mb})$	147.6(1)
$\text{O}(1\text{m})\text{--Na}(1)\text{--O}(1\text{mb})$	83.6(1)	$\text{O}(1)\text{--Na}(2)\text{--O}(1\text{mc})$	127.6(1)
$\text{O}(1)\text{--Na}(2)\text{--O}(1\text{b})$	70.0(1)	$\text{Fe}(1)\text{--O}(1)\text{--Na}(2)$	87.6(1)
$\text{O}(1\text{m})\text{--Na}(2)\text{--O}(1\text{mb})$	83.0(1)	$\text{Na}(1)\text{--O}(1\text{m})\text{--Na}(2)$	79.8(1)
$\text{O}(1)\text{--Na}(2)\text{--O}(1\text{m})$	89.7(1)		

Symmetry transformations used to generate equivalent atoms: a  $x - y$ ,  $x, -z$ ; b  $-x + y, -x, z$ ; c  $-y, x - y, z$ .

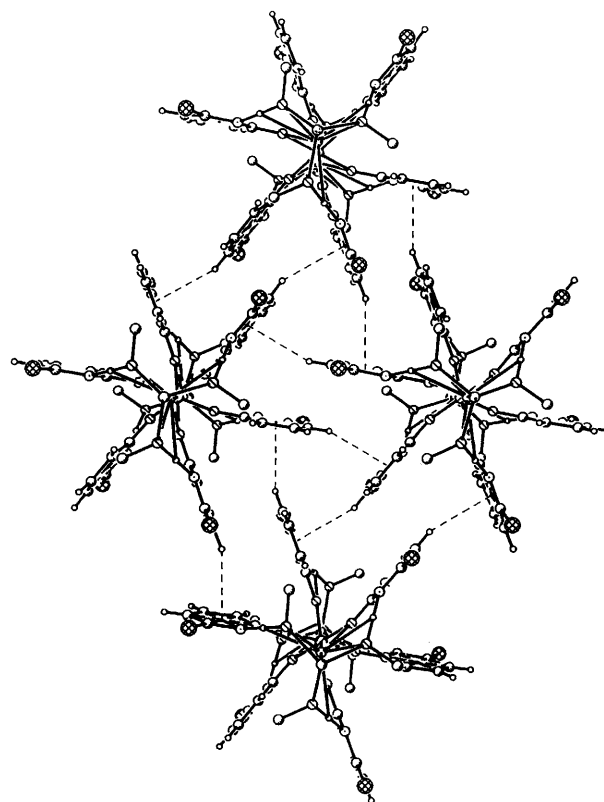


**Fig. 2** Packing diagram for complex **1**

X-ray diffraction studies were grown from  $\text{thf}\text{--MeOH}$  mixtures at 293 and 273 K, respectively. Selected bond distances and angles for **2** are given in Table 2 and those for **3** in Table 3.

The molecular structures of complexes **2** (Fig. 3) and **3** (Fig. 4) consist of similar dimeric units with the bidentate ligands occupying similar positions in both structures. Each dimer unit is produced by inverting the asymmetric unit  $\text{Fe}(\text{chp})_2(\text{L}\text{--L})$

( $\text{L}\text{--L} = \text{dmbipy } \mathbf{2}$  or  $\text{phen } \mathbf{3}$ ) about a crystallographic inversion centre on the centroid of the  $\text{Fe}_2\text{O}_2$  core (Figs. 3 and 4). The two crystallographically equivalent iron(III) atoms are bridged in both complexes by two methoxide groups and terminally bound by two  $\text{chp}$  ligands and one  $\text{L}\text{--L}$  ligand to complete an approximately octahedral environment. The  $\text{chp}$  ligands coordinate to iron *via* the exocyclic oxygen atom while one non-

**Table 2** Selected bond distances (Å) and angles (°) for complex 2

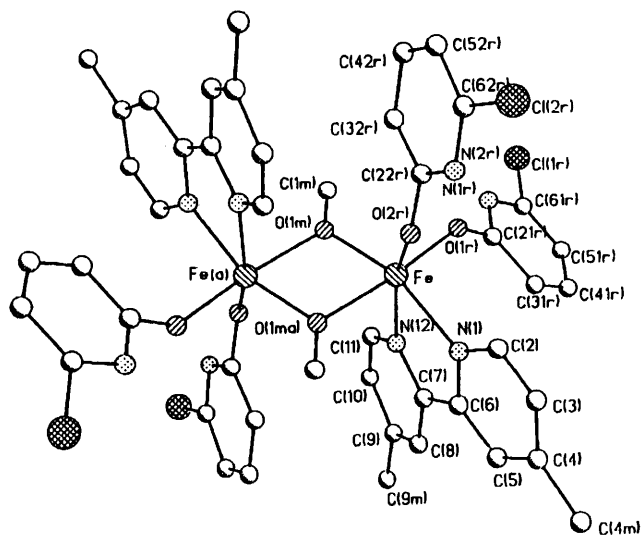
Fe–O(2r)	1.912(10)	Fe–N(12)	2.179(13)
Fe–O(1r)	1.936(12)	Fe(a)–O(1m)	2.045(12)
Fe–O(1m)	1.987(11)	Fe...Fe(a)	3.194(10)
Fe–O(1ma)	2.045(12)	N(2r)...O(2s)	2.831(10)
Fe–N(1)	2.192(13)		
O(2r)–Fe–O(1r)	97.5(5)	O(1m)–Fe–N(12)	95.1(5)
O(2r)–Fe–O(1m)	103.1(4)	O(1ma)–Fe–N(12)	87.5(5)
O(1r)–Fe–O(1m)	95.4(5)	O(2r)–Fe–N(1)	86.0(5)
O(2r)–Fe–O(1ma)	89.3(5)	O(1r)–Fe–N(1)	98.1(5)
O(1r)–Fe–O(1ma)	169.4(5)	O(1m)–Fe–N(1)	162.6(5)
O(1m)–Fe–O(1ma)	75.3(4)	O(1ma)–Fe–N(1)	90.2(5)
O(2r)–Fe–N(12)	160.1(5)	N(12)–Fe–N(1)	74.3(5)
O(1r)–Fe–N(12)	88.5(5)	Fe–O(1m)–Fe(a)	104.7(4)

Symmetry transformations used to generate equivalent atoms:  $a - x + 2, -y, -z + 1$ .

**Table 3** Selected bond distances (Å) and angles (°) for complex 3

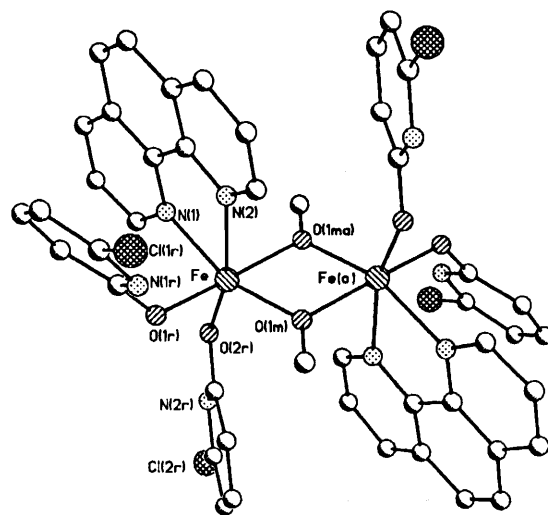
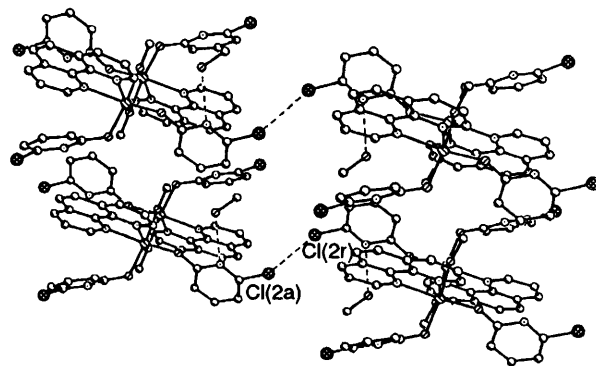
Fe–O(2r)	1.924(3)	Fe–N(2)	2.193(4)
Fe–O(1r)	1.948(3)	Fe(a)–O(1m)	2.045(3)
Fe–O(1m)	1.948(3)	Fe...Fe(a)	3.153(3)
Fe–O(1ma)	2.045(3)	N(2r)...O(1s)	2.905(3)
Fe–N(1)	2.184(4)	N(2r)...H(1s)	1.901(4)
O(2r)–Fe–O(1r)	93.2(1)	O(1m)–Fe–N(2)	92.7(1)
O(2r)–Fe–O(1m)	104.8(1)	O(1ma)–Fe–N(2)	87.5(1)
O(1r)–Fe–O(1m)	100.6(1)	O(2r)–Fe–N(1)	86.9(1)
O(2r)–Fe–O(1ma)	93.9(1)	O(1r)–Fe–N(1)	92.3(1)
O(1r)–Fe–O(1ma)	172.6(1)	O(1m)–Fe–N(1)	161.9(1)
O(1m)–Fe–O(1ma)	75.7(1)	O(1ma)–Fe–N(1)	90.0(1)
O(2r)–Fe–N(2)	162.3(1)	N(2)–Fe–N(1)	75.4(1)
O(1r)–Fe–N(2)	86.3(1)	Fe–O(1m)–Fe(a)	104.3(1)

Symmetry transformations used to generate equivalent atoms:  $a - x + 1, -y + 1, -z + 1$ .

**Fig. 3** Molecular structure of complex 2 including the atom numbering scheme

co-ordinating ring nitrogen in the chp ligand on each iron is involved in hydrogen bonding with methanol solvent of crystallisation (not shown in figures). In 3 the quality of the X-ray data allowed the location of the hydrogen atom in MeOH with the N...H–OMe and MeO–H distances being 1.901(4) and 1.013(3) Å respectively.

The Fe...Fe separations [3.194(10) 2, 3.153(3) Å 3], the Fe–O–Fe angles [104.7(4) 2, 104.3(1)° 3] and the Fe–OMe bond lengths [1.987(11), 2.045(12) 2; 1.948(3), 2.045(3) Å 3] are in the mid-range for structures of similar type.<sup>1,2</sup> As with previous examples, the Fe–N distances [2.192(13), 2.179(13) 2; 2.184(4), 2.193(4) 3] are noticeably longer than the Fe–O(1m), –O(1ma),

**Fig. 4** Molecular structure of complex 3 including the atom numbering scheme**Fig. 5** Packing diagram for complex 3

–O(1r) and –O(2r) bond lengths, a feature that has been attributed to the greater affinity of iron for oxygen.<sup>21</sup>

In both complexes 2 and 3 hydrogen bonding is restricted to MeOH solvate interactions with a ring nitrogen of one chp ligand per iron. Intermolecular interactions between the planar dmbipy (2) and phen (3) ligands are noticeably lacking. There is, however, a contact between chlorides on the chp rings in adjacent molecules in 3 of 3.342 Å (Fig. 5) whereas in 2 the closest Cl...Cl contact is 3.960 Å. The nature of this type of interaction is unclear but has been observed in other transition-metal complexes with chp ligands.<sup>8</sup>

Attempts to convert complex 1 into 2 or 3 by addition of dmbipy or phen were unsuccessful and, similarly, the addition of equimolar equivalents of sodium methoxide and Hchp to 2 or 3 did not afford crystalline 1.

Iron complexes containing co-ordinated deprotonated pyridone ligands are rare. Indeed, only two have been reported in which protonated pyridones co-ordinate, [Fe(Hxhp)<sub>6</sub>][NO<sub>3</sub>]<sub>3</sub> (Hxhp = 2-pyridone or 6-methyl-2-pyridone).<sup>9,10</sup> It is noteworthy that in these latter complexes the Fe–O(pyridone) distances [range 1.988(4)–2.003(4) Å] are longer than the iron–oxo(pyridonate) distances in 2 [1.912(10), 1.936(12) Å] and 3 [1.924(3), 1.948(3) Å] but comparable with the corresponding distances in 1 [1.999(2) Å]. Apart from the heptadecanuclear complex [Fe<sub>17</sub>O<sub>15</sub>(OH)<sub>6</sub>(chp)<sub>12</sub>(phen)<sub>8</sub>(OMe)<sub>3</sub>]<sup>11</sup> recently reported by our group, complexes 1–3 represent the first entries into the chemistry of iron bound to deprotonated pyridone ligands.

#### (b) Magnetic studies of complexes 1–3

The magnetic properties of complexes 1–3 have been studied over the temperature range 1.8–280 K in an applied field of 1000

**Table 4** Structural and magnetic parameters for known dialkoxo-bridged iron(III) complexes

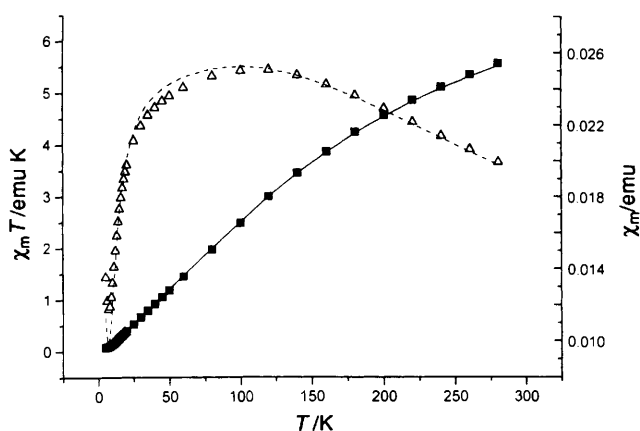
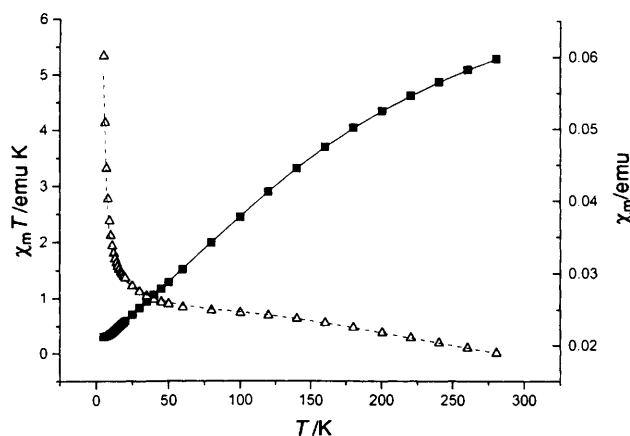
Formula	$-J/\text{cm}^{-1}$	$\text{Fe} \cdots \text{Fe}/\text{\AA}$	$\text{Fe}-\text{O}-\text{Fe}/^\circ$	$P^a/\text{\AA}$	Ref.
$[\text{FeL}^1]_2[\text{ClO}_4]_2$ <sup>b</sup>	5.2	3.180(3)	103.8(2)	2.021(5)	2(a)
$[\text{Fe}_2\text{L}^2(\text{Him})_4][\text{BF}_4]_2$ <sup>c</sup>	1.5	3.117(2)	96.3(2)	2.092(5)	2(b)
$[\text{Fe}_2\text{L}^3(\text{OMe})_2\text{Cl}_2]$ <sup>d</sup>	16.3	3.106(7)	103(1)	1.99(2)	2(c)
$[\text{Fe}_2\text{L}^4(\text{OMe})\text{Cl}_2]$ <sup>e</sup>	8.0	3.139(5)	100(1)	2.01(2)	2(d)
$[\text{Fe}_2\text{L}^5_2(\text{OMe})_2]$ <sup>f</sup>	10.9	3.168(1)	104.58(5)	2.002(1)	2(e)
$[\text{Fe}_2\text{L}^3(\text{OEt})_2\text{Cl}_2]$	15.4	3.144(1)	104.3(1)	1.991(3)	2(f)
$[\text{Fe}_2(\text{acac})_4(\text{OEt})_2]$	11.0	3.116(1)	103.6(3)	1.982(4)	2(f)
$[\text{Fe}_2\text{L}^6_2]$ <sup>g</sup>	-1.2	3.063(1)	97.06(9)	2.044(2)	2(g)
$[\text{PHBu}^i_3]_2[\text{Fe}_2(\text{OEt})_2\text{Cl}_6]$	24.6	3.177(2)	107.0(3)	1.976(6)	2(h)
$[\text{Fe}_2\text{L}^7_2(\text{CH}_2\text{Ph})_2][\text{ClO}_4]_2$ <sup>h</sup>	20.5	3.21(1)	107.4(6)	2.00(1)	2(i)
$[\text{Fe}_2\text{L}^8(\text{OMe})\text{Cl}_2(\text{MeOH})]$ <sup>i</sup>	10.6	3.140(2)	102.7(1)	2.009(2)	2(j)
$[\text{Fe}_2(\text{acac})_4(\text{OCH}_2\text{CF}_3)_2]$	6.5	3.154(2)	102.6(2)	2.022(3)	2(k)
$[\text{Fe}_2\text{L}^9(\text{H}_2\text{O})_2]$ <sup>j</sup>	13.4	3.119(1)	104.3(1)	1.976(3)	2(l)
$[\text{Fe}_2(\text{OMe})_2(\text{chp})_4(\text{dmbipy})_2]$ <b>2</b>	26.8	3.194(10)	104.7(4)	2.016(12)	This work
$[\text{Fe}_2(\text{OMe})_2(\text{chp})_4(\text{phen})_2]$ <b>3</b>	28.6	3.153(3)	104.3(1)	1.997(3)	This work

<sup>a</sup> Defined as one half of the shortest superexchange pathway (see ref. 13). <sup>b</sup>  $\text{H}_2\text{L}^1 = \alpha,3$ -Dihydroxy- $\beta$ -{[3-hydroxy-5-(hydroxymethyl)-2-methyl-4-pyridyl]methylamino}-5-(hydroxymethyl)- $\alpha,2$ -dimethylpyridine-4-propanoic acid. <sup>c</sup>  $\text{H}_2\text{L}^2 = 11,23$ -Dimethyl-3,7,15,19-tetraazatricyclo-[19.3.1.1]hexacos-2,7,9,11,13(26),14,19,21(25),22,24-decaene-25,26-diol; Him = imidazole. <sup>d</sup>  $\text{H}_2\text{L}^3 = 1,4$ -Piperazinebis(*N*-ethylenesalicylaldimine). <sup>e</sup>  $\text{H}_3\text{L}^4 =$  Trisalicylideneetriethylenetetramine. <sup>f</sup>  $\text{H}_2\text{L}^5 = \text{Me}_2\text{CHN}(\text{OH})\text{C}(\text{O})(\text{CH}_2)_5\text{C}(\text{O})\text{N}(\text{OH})\text{CHMe}_2$ . <sup>g</sup>  $\text{H}_3\text{L}^6 = 2$ -[bis(salicylidene amino)methyl]phenol. <sup>h</sup>  $\text{L}^7 = 2$ -[Bis(benzimidazol-2-ylmethyl)amino]ethanol. <sup>i</sup>  $\text{H}_3\text{L}^8 = N,N'$ -Bis(salicylidene)-1,3-diaminopropan-2-ol. <sup>j</sup>  $\text{H}_3\text{L}^9 = \text{N}(\text{CH}_2\text{CO}_2\text{H})_2(\text{CH}_2\text{CH}_2\text{OH})$ .

**Table 5** Experimental data for the X-ray diffraction studies of complexes 1–3

Compound	1	2	3
Formula	$\text{C}_{36}\text{H}_{42}\text{Cl}_6\text{Fe}_6\text{Na}_3\text{O}_{12} \cdot 2\text{C}_4\text{H}_8\text{O}$	$\text{C}_{46}\text{H}_{42}\text{Cl}_4\text{Fe}_2\text{N}_8\text{O}_6 \cdot 2\text{CH}_3\text{OH}$	$\text{C}_{46}\text{H}_{34}\text{Cl}_4\text{Fe}_2\text{N}_8\text{O}_6 \cdot 2\text{CH}_3\text{OH}$
<i>M</i>	1232.5	1120.4	1112.4
Crystal system	Trigonal	Monoclinic	Triclinic
Space group	$P\bar{3}$	$P2_1/c$	$P\bar{1}$
<i>a</i> /Å	11.601(1)	8.665(6)	9.107(5)
<i>b</i> /Å	11.601(1)	11.740(7)	10.545(7)
<i>c</i> /Å	12.129(1)	24.90(2)	13.885(10)
$\alpha/^\circ$			81.65(4)
$\beta/^\circ$		92.89(5)	77.97(4)
$\gamma/^\circ$			66.14(3)
<i>U</i> /Å <sup>3</sup>	1414	2530	1190
No. reflections	10	50	15
2 $\theta$ range/ $^\circ$	30–32	10–26	24–26
<i>Z</i>	1 <sup>a</sup>	2	1
<i>D<sub>c</sub></i> /g cm <sup>-3</sup>	1.448	1.471	1.552
<i>F</i> (000)	637	1156	5700
Crystal size/mm	0.66 × 0.47 × 0.47	0.35 × 0.12 × 0.09	0.47 × 0.31 × 0.08
Crystal habit	Red hexagonal prism	Red needle	Red plate
$\mu/\text{mm}^{-1}$	0.638	0.845	0.900
Unique data	1661	2327	3119
Observed data [ <i>I</i> > 2 $\sigma$ ( <i>I</i> )]	1406	1155	2248
Parameters	142	181	318
Maximum $\Delta/\sigma$ ratio	+0.058	+0.004	-0.090
<i>R</i> <sub>1</sub> , <i>wR</i> <sub>2</sub> <sup>b</sup>	0.0454, 0.1246	0.0928, 0.2609	0.0432, 0.1042
Weighting, <i>c w</i> <sup>-1</sup>	$[\sigma^2(F_o^2) + (0.067P)^2 + 1.71P]$	$[\sigma^2(F_o^2) + (0.078P)^2 + 22.68P]$	$[\sigma^2(F_o^2) + (0.077P)^2]$
<i>S</i>	1.039	1.030	0.989
Largest residue/e Å <sup>-3</sup>	+0.712, -0.527	+0.503, -0.533	+0.345, -0.451

<sup>a</sup> For the stoichiometric unit of the polymer. <sup>b</sup> SHELXL 93. <sup>17</sup>  $c P = \frac{1}{3}(2F_c^2 + F_o^2)$ .

**Fig. 6** Plots of  $\chi_m$  ( $\Delta$ ) and  $\chi_m T$  ( $\blacksquare$ ) as functions of *T* for complex 2. — and — —, calculated curves**Fig. 7** Plots of  $\chi_m$  and  $\chi_m T$  as functions of *T* for complex 3. — and — —, calculated curves

G (0.1 T). For **1** a problem arises in that the elemental analysis suggests loss of solvent from the structure, therefore we cannot be certain that the polymeric nature of the material is maintained. The magnetic moment for **1** is invariant at  $5.9 \mu_B$  per iron from 280 down to 40 K. Below this temperature there is a slight fall in the moment down to  $5.3 \mu_B$  per iron at low temperature. This fall has two possible causes, either a very weak antiferromagnetic exchange between iron(III) centres, or zero-field splitting of the  $S = \frac{5}{2}$  ground state. We favour the latter explanation and the compound is therefore best described as a simple paramagnet.

For the two dinuclear complexes the behaviour is consistent with antiferromagnetic exchange between the two iron centres. Their magnetic properties can be modelled using standard procedures for an isotropic Heisenberg Hamiltonian<sup>12</sup>  $\mathcal{H} = -2JS_1S_2$  where  $S_1$  and  $S_2$  are the spin operators for the two iron centres. For  $[\text{Fe}_2(\mu\text{-OMe})_2(\text{chp})_4(\text{dmbipy})_2]\cdot 2\text{MeOH}$  **2** a good fit to the observed data is achieved with  $J = -26.8 \text{ cm}^{-1}$ . For  $[\text{Fe}_2(\mu\text{-OMe})_2(\text{chp})_4(\text{phen})_2]\cdot 2\text{MeOH}$  **3** a moderate fit can be achieved with  $J = -28.6 \text{ cm}^{-1}$ , however, there is a marked divergence below 20 K. A much better match is obtained if we allow for the presence of a monomeric impurity, and the best fit occurs with 6.5% of an iron monomer. This result led us to re-examine the data for **2** and we found that here too an improved fit resulted if a 1.5% monomer impurity was included in the model. In both cases it is possible that this impurity is the polymeric complex **1**. Plots of  $\chi_m/T$  and  $\chi_m T/T$  are shown for **2** and **3** in Fig. 6 and 7 respectively.

Studies of a number of hydroxo- and alkoxo-bridged dimeric iron(III) complexes have been reported.<sup>1,2</sup> The exchange-interaction parameters in these previous examples have ranged from  $+1.2$  to  $-25 \text{ cm}^{-1}$ . The values found here are therefore consistent with, but at the upper end of, the range. No correlation between the magnetic properties and the structural features has yet been established in these systems, although in related ( $\mu$ -oxo)-bridged iron(III) complexes Gorun and Lippard<sup>13</sup> have proposed a correlation between  $J$  and the shortest superexchange pathway. In Table 4 we list the examples of alkoxo-bridged species in which both structures and low-temperature magnetic studies have been performed, including  $J$  values and three structural parameters. No striking correlation between any geometric parameters and the magnitude of the exchange coupling is observed. In general,  $J$  increases with an increased angle at the bridging O atom in planar structures and with a decrease in the shortest superexchange pathway.

## Conclusion

We have prepared three new polynuclear iron(III) pyridonate complexes. Complexes **2** and **3** contain Fe–O(R)–Fe units and exhibit weak antiferromagnetic exchange interactions. In the unusual heterobimetallic complex **1**, in which the iron(III) centres are separated by three sodium atoms, paramagnetic behaviour is observed. None of the complexes has the chp ligands adopting 1,3-bridging modes, instead these ligands act terminally through the oxygen atom in **2** and **3**, while in the presence of an alkali metal as in **1** they bridge iron and sodium in a 1,1 bonding mode.

The nature of the substituent at the 6 position of the pyridonate functionality has been previously found to effect its bonding mode and we are currently interested in varying this substituent so as to encourage the ring nitrogen to participate in the bonding.

## Experimental

Anhydrous iron(III) chloride, sodium methoxide and 6-chloro-2-pyridone (Hchp), 4,4'-dimethyl-2,2'-bipyridine and 1,10-phenanthroline were obtained from Aldrich and used without further purification. The complex  $[\text{NEt}_4]_2[\text{Fe}_2\text{Cl}_6\text{O}]$  was syn-

**Table 6** Atomic coordinates ( $\times 10^4$ ) for complex **1**

Atom	x	y	z
Fe(1)	0	0	0
Na(1)	0	0	5000
Na(2)	0	0	2488(1)
O(1)	-825(2)	717(2)	1041(2)
N(1)	-2318(2)	892(2)	2115(2)
Cl(1)	-3869(1)	1084(1)	3558(1)
C(12r)	-1840(3)	901(3)	1091(2)
C(13r)	-2424(3)	1140(3)	162(2)
C(14r)	-3487(3)	1333(3)	309(3)
C(15r)	-3991(3)	1293(3)	1354(3)
C(16r)	-3350(3)	1079(3)	2204(2)
O(1m)	1766(2)	524(2)	3753(2)
C(1m)	2294(4)	-353(5)	3742(3)
O(1s)	-6667	-3333	1908(4)
C(1s)	-5807(18)	-2190(11)	2599(8)
C(2s)	-6131(38)	-2632(22)	3740(10)
C(1s')	-7391(20)	-4501(10)	2596(8)
C(2s')	-7092(82)	-4058(26)	3745(11)

**Table 7** Atomic coordinates ( $\times 10^4$ ) for complex **2**

Atom	x	y	z
Fe	9 880(3)	1 357(2)	4 989(1)
N(1)	7 784(15)	2 368(11)	4 822(5)
C(2)	7 499(21)	2 955(15)	4 377(7)
C(3)	6 149(17)	3 510(14)	4 260(6)
C(4)	5 012(19)	3 552(15)	4 634(6)
C(4m)	3 533(20)	4 163(15)	4 540(7)
C(5)	5 336(21)	2 961(15)	5 123(7)
C(6)	6 688(18)	2 370(14)	5 212(6)
C(7)	7 187(20)	1 818(15)	5 713(6)
C(8)	6 281(19)	1 715(13)	6 167(6)
C(9)	6 832(17)	1 293(14)	6 622(6)
C(9m)	5 867(20)	1 145(16)	7 101(6)
C(10)	8 359(19)	879(14)	6 661(7)
C(11)	9 193(22)	930(15)	6 200(7)
N(12)	8 677(14)	1 371(12)	5 737(5)
N(1r)	12 508(15)	3 301(11)	6 005(5)
O(1r)	11 196(13)	2 564(10)	5 279(5)
Cl(1r)	14 354(6)	4 086(4)	6 779(2)
C(21r)	11 227(21)	3 273(15)	5 678(7)
C(31r)	9 971(23)	4 027(16)	5 772(7)
C(41r)	10 123(22)	4 763(17)	6 195(7)
C(51r)	11 401(19)	4 778(15)	6 533(7)
C(61r)	12 603(22)	4 043(16)	6 401(7)
N(2r)	11 049(16)	2 249(12)	3 444(5)
O(2r)	10 271(12)	1 572(10)	4 247(4)
Cl(2r)	11 603(7)	3 035(6)	2 509(2)
C(22r)	11 469(21)	1 776(15)	3 943(7)
C(32r)	12 943(18)	1 372(15)	4 059(6)
C(42r)	14 104(20)	1 553(15)	3 693(6)
C(52r)	13 691(21)	2 042(15)	3 219(7)
C(62r)	12 172(22)	2 398(16)	3 117(7)
O(1m)	11 311(11)	99(10)	5 209(4)
C(1m)	12 654(19)	189(16)	5 545(6)
O(2s)	2 097(15)	7 140(14)	1 918(6)
C(2s)	2 078(26)	6 194(20)	2 260(8)

thesised by a literature method.<sup>7</sup> Solvents were dried by conventional methods and distilled under nitrogen prior to use.

Mass spectra were attempted using fast atom bombardment (FAB) on samples in a 3-nitrobenzyl alcohol matrix. Infrared (IR) spectra were recorded on a Perkin-Elmer Paragon 1000 FT-IR spectrometer as Nujol mulls with KBr or NaCl discs. Microanalyses were performed at the University of Edinburgh Micro-Analytical Laboratory.

## Preparations

$[\{\text{Fe}(\mu\text{-chp})_2\text{Na}_3(\mu\text{-MeOH})_6\cdot 2\text{thf}\}_n]$  **1**. (a) Sodium methoxide (0.199 g, 3.69 mmol) and Hchp (0.478 g, 3.69 mmol) were added to a solution of anhydrous iron(III) chloride (0.100 g, 0.62 mmol) in MeOH (30 cm<sup>3</sup>) and stirred for 24 h at room

**Table 8** Atomic coordinates ( $\times 10^4$ ) for complex 3

Atom	x	y	z
Fe	4543(1)	6470(1)	5384(1)
O(1m)	3573(3)	5160(3)	5288(2)
C(1m)	2000(5)	5204(5)	5740(4)
N(1r)	1828(4)	7332(4)	7777(3)
O(1r)	2730(4)	7851(3)	6167(2)
Cl(1r)	788(2)	6491(2)	9540(1)
C(12r)	2550(5)	8046(5)	7106(3)
C(13r)	3152(6)	8932(5)	7413(4)
C(14r)	3017(6)	9035(5)	8402(4)
C(15r)	2307(6)	8281(5)	9092(4)
C(16r)	1715(5)	7478(5)	8714(3)
N(2r)	3776(5)	8697(4)	2688(3)
O(2r)	4275(4)	7647(3)	4184(2)
Cl(2r)	3543(2)	9871(1)	918(1)
C(22r)	3260(6)	8115(5)	3557(3)
C(23r)	1712(5)	8047(5)	3749(4)
C(24r)	749(6)	8545(5)	3044(4)
C(25r)	1265(6)	9150(5)	2147(4)
C(26r)	2778(6)	9167(5)	2033(3)
N(1)	6262(4)	7329(4)	5593(3)
N(2)	5318(4)	5471(4)	6792(3)
C(1)	6646(6)	8289(5)	5012(4)
C(2)	7638(5)	8883(5)	5249(3)
C(3)	8254(6)	8453(5)	6106(3)
C(4)	7823(5)	7460(5)	6756(4)
C(5)	8345(6)	6990(5)	7693(4)
C(6)	7833(6)	6086(6)	8307(4)
C(7)	6801(6)	5532(5)	8036(3)
C(8)	6180(6)	4623(5)	8659(4)
C(9)	5160(6)	4175(5)	8348(4)
C(10)	4758(5)	4619(5)	7405(3)
C(11)	6316(5)	5933(5)	7109(3)
C(12)	6831(5)	6921(5)	6466(3)
C(1s)	8156(7)	7275(6)	1725(4)
O(1s)	7255(4)	7804(4)	2634(3)

temperature to give a red precipitate. The solvent was removed under reduced pressure and thf (15 cm<sup>3</sup>) added to the red residue. This solution was stirred for 15 min, filtered through a Celite plug and left to stand at room temperature overnight to give dark red crystals of complex 1 (0.299 g, 40%). Larger crystals of 1, suitable for a single-crystal X-ray structure analysis, were obtained on prolonged standing of a thf solution at 253 K (Found: C, 40.30; H, 2.45; N, 9.15. C<sub>36</sub>H<sub>42</sub>Cl<sub>6</sub>FeN<sub>6</sub>Na<sub>3</sub>O<sub>12</sub>·2C<sub>2</sub>H<sub>6</sub>O requires C, 42.85; H, 4.70; N, 6.80%. C<sub>30</sub>H<sub>18</sub>Cl<sub>6</sub>FeN<sub>6</sub>Na<sub>3</sub>O<sub>6</sub>·1CH<sub>3</sub>OH requires C, 40.10; H, 2.35; N, 9.05%). IR (KBr, cm<sup>-1</sup>) 3408 ν(MeO–H), 1645, 1590, 1545, 1436, 1314, 1155, 990, 920, 788, 722, 697 and 604. No significant peaks were observed by FAB mass spectroscopy.

(b) Sodium methoxide (0.359 g, 6.66 mmol) and Hchp (0.862 g, 6.66 mmol) were added to a solution of [NEt<sub>4</sub>]<sub>2</sub>[Fe<sub>2</sub>Cl<sub>6</sub>O] (0.500 g, 0.83 mmol) in MeOH (75 cm<sup>3</sup>) and stirred for 24 h at room temperature to give a red precipitate. Crystals of complex 1 were obtained as in (a) above.

[Fe<sub>2</sub>(μ-OMe)<sub>2</sub>(chp)<sub>4</sub>(dmbipy)<sub>2</sub>]-2MeOH 2. Sodium methoxide (0.133 g, 2.46 mmol), Hchp (0.319 g, 2.46 mmol) and dmbipy (0.113 g, 0.62 mmol) were added to a solution of anhydrous iron(III) chloride (0.100 g, 0.62 mmol) in MeOH (30 cm<sup>3</sup>) and stirred for 24 h at room temperature to give a red precipitate. The solvent was removed under reduced pressure and thf (15 cm<sup>3</sup>) and MeOH (5 cm<sup>3</sup>) added to the red residue. After stirring for 15 min the solution was filtered through a Celite plug and left at 273 K overnight to give red crystals of complex 2 (0.448 g, 65%) (Found: C, 51.15; H, 4.15; N, 9.85. C<sub>46</sub>H<sub>42</sub>Cl<sub>4</sub>Fe<sub>2</sub>N<sub>8</sub>O<sub>6</sub>·2CH<sub>3</sub>OH requires C, 51.45; H, 4.45; N, 10.00%). IR (KBr, cm<sup>-1</sup>) 3312 [ν(MeO–H)], 1615, 1582, 1536, 1329, 1150, 1136, 1035, 1022, 978, 923, 859, 843, 824, 788, 728, 696, 616, 552, 521 and 483. No significant peaks were observed in the FAB mass spectrum.

[Fe<sub>2</sub>(μ-OMe)<sub>2</sub>(chp)<sub>4</sub>(phen)<sub>2</sub>]-2MeOH 3. Sodium methoxide (0.133 g, 2.46 mmol), Hchp (0.319 g, 2.46 mmol) and phen (0.111 g, 0.62 mmol) were added to a solution of anhydrous iron(III) chloride (0.100 g, 0.62 mmol) in MeOH (30 cm<sup>3</sup>) and stirred for 24 h at room temperature to give a red precipitate. The solvent was removed under reduced pressure and thf (15 cm<sup>3</sup>) and MeOH (5 cm<sup>3</sup>) added to the red residue. After stirring for 15 min the solution was filtered through a Celite plug and left at 293 K overnight to give red crystals of complex 3 (0.404 g, 59%) (Found: C, 52.15; H, 3.65; N, 10.00. C<sub>46</sub>H<sub>34</sub>Cl<sub>4</sub>Fe<sub>2</sub>N<sub>8</sub>O<sub>6</sub>·2CH<sub>3</sub>OH requires C, 51.80; H, 3.80; N, 10.05%). IR (KBr, cm<sup>-1</sup>) 3363 [ν(MeOH)], 1582, 1537, 1342, 1146, 1106, 1033, 984, 918, 849, 790, 726, 632 and 488. No significant peaks were observed in the FAB mass spectrum.

### Crystal structure determinations

Crystal data and data collection and refinement parameters for compounds 1–3 are given in Table 5 and atomic coordinates in Tables 6–8.

**Data collection and processing.** Data were collected on a Stöe Stadi-4 four-circle diffractometer equipped with an Oxford Cryosystems low-temperature device<sup>14</sup> operating at 150 K, with graphite-monochromated Mo-K $\alpha$  radiation ( $\lambda$  0.710 73 Å) and  $\omega$ -2 $\theta$  scans using on-line profile fitting.<sup>15</sup> Data were corrected for Lorentz and polarisation factors and for absorption ( $\psi$ -scans).

**Structure analysis and refinement.** Structure 1 was solved by the heavy-atom method, 2 and 3 by direct methods using SHELXS 86.<sup>16</sup> All non-hydrogen atoms were located from subsequent  $\Delta F$  maps and refined anisotropically.

Hydrogen atoms in complex 2 were initially included in idealised positions (C–H 0.96 Å for ring hydrogens and 0.98 Å for methyl hydrogens; O–H 0.84 Å) and, during subsequent refinement, allowed to ride on their parent atoms with isotropic thermal parameters equal to 1.2U<sub>eq</sub>(C) Å<sup>2</sup> for ring carbons and 1.5U<sub>eq</sub>(C or O) for methyl and hydroxyl groups. Hydrogen-bonded methanolic hydrogens in 1 and 3 were located in  $\Delta F$  maps and refined with fixed isotropic thermal parameters ( $U = 0.08$  Å<sup>2</sup> for 1, 0.05 Å<sup>2</sup> for 3).

For complex 1 the thf molecule of crystallisation was modelled as being disordered about a crystallographic three-fold axis, and refined with C–O and C–C bond lengths restrained to chemically reasonable values. All non-H atoms were refined anisotropically with rigid bond and similarity restraints on the constituent atoms of the thf molecule.

Complete atomic coordinates, thermal parameters and bond lengths and angles have been deposited at the Cambridge Crystallographic Data Centre. See Instructions for Authors, *J. Chem. Soc., Dalton Trans.*, 1996, Issue 1.

### Magnetic measurements

Variable-temperature magnetic measurements on complexes 1–3 in the region 1.8–280 K were made using a SQUID magnetometer (Quantum Design) with samples sealed in gelatine capsules. In all cases diamagnetic corrections for the sample holders were applied to the data. Diamagnetic corrections for the samples were determined from Pascal's constants<sup>18</sup> and literature values.<sup>19,20</sup> The observed and calculated data were refined using in-house software.<sup>21</sup>

### Acknowledgements

We thank the EPSRC for funding a studentship (to C. M. G.), a post-doctoral fellowship (to S. P.) and for funding for a diffractometer and SQUID susceptometer. We are also grateful to the Leverhulme Trust for a post-doctoral fellowship (to G. A. S.).

## References

- 1 D. M. Kurtz, *Chem. Rev.*, 1990, **90**, 585; J. B. Vincent, G. L. Olivier-Lilley and B. A. Averill, *Chem. Rev.*, 1990, **90**, 1447.
- 2 (a) G. J. Long, J. T. Wroblewski, R. V. Thundathil, D. M. Sparlin and E. O. Schlemper, *J. Am. Chem. Soc.*, 1980, **102**, 6040; (b) C. L. Spiro, S. L. Lambert, T. J. Smith, E. N. Duesler, R. R. Gagné and D. N. Hendrickson, *Inorg. Chem.*, 1981, **20**, 1229; (c) B. Chiari, O. Piovesana, T. Tarantelli and P. F. Zanazzi, *Inorg. Chem.*, 1982, **21**, 1396; (d) B. Chiari, O. Piovesana, T. Tarantelli and P. F. Zanazzi, *Inorg. Chem.*, 1982, **21**, 2444; (e) S. J. Barclay, P. E. Riley and K. N. Raymond, *Inorg. Chem.*, 1984, **23**, 2005; (f) B. Chiari, O. Piovesana, T. Tarantelli and P. F. Zanazzi, *Inorg. Chem.*, 1984, **23**, 3398; (g) B. S. Snyder, G. S. Patterson, A. J. Abrahamson and R. H. Holm, *J. Am. Chem. Soc.*, 1989, **111**, 5214; (h) R. D. Walker and R. Poli, *Inorg. Chem.*, 1990, **29**, 756; (i) S. Ménage and L. Que, jun., *Inorg. Chem.*, 1990, **29**, 4293; (j) G. D. Fallon, A. Markiewicz, K. S. Murray and T. Quach, *J. Chem. Soc., Chem. Commun.*, 1991, 198; (k) M. Leluk, B. Jezowska-Trzebiatowska and T. Lis, *Polyhedron*, 1992, **11**, 1923; (l) A. K. Powell, S. L. Heath, D. Gatteschi, L. Pardi, R. Sessoli, G. Spina, F. Del Giallo and F. Pieralli, *J. Am. Chem. Soc.*, 1995, **117**, 2491.
- 3 W. H. Armstrong, A. Spool, G. C. Papaefthymiou, R. B. Frankel and S. J. Lippard, *J. Am. Chem. Soc.*, 1984, **106**, 3653; K. Wieghardt, J. Pohl and W. Gebert, *Angew. Chem., Int. Ed. Engl.*, 1983, **22**, 727; J. B. Vincent, H. C. Huffman, G. Christou, Q. Li, M. A. Nanny, D. N. Hendrickson, R. H. Fong and R. H. Fish, *J. Am. Chem. Soc.*, 1988, **110**, 6898; R. H. Beer, W. B. Tolman, S. G. Bott and S. J. Lippard, *Inorg. Chem.*, 1989, **28**, 4559.
- 4 M. Kato, Y. Yamada, T. Inagaki, W. Mori, K. Sakai, T. Tsubomura, M. Sato and S. Yano, *Inorg. Chem.*, 1995, **34**, 2645 and refs. therein.
- 5 J. M. Rawson and R. E. P. Winpenny, *Coord. Chem. Rev.*, 1995, **139**, 313.
- 6 A. J. Blake, C. M. Grant, S. Parsons, J. M. Rawson, G. A. Solan and R. E. P. Winpenny, *J. Chem. Soc., Dalton Trans.*, 1995, 2311.
- 7 W. H. Armstrong and S. J. Lippard, *Inorg. Chem.*, 1985, **24**, 981.
- 8 P. E. Y. Milne, Ph. D. Thesis, The University of Edinburgh, 1993.
- 9 D. M. L. Goodgame, D. J. Williams and R. E. P. Winpenny, *Inorg. Chim. Acta*, 1989, **166**, 159.
- 10 A. J. Blake, R. O. Gould, C. M. Grant, P. E. Y. Milne and R. E. P. Winpenny, *Polyhedron*, 1994, **13**, 187.
- 11 S. Parsons, G. A. Solan and R. E. P. Winpenny, *J. Chem. Soc., Chem. Commun.*, 1995, 1987.
- 12 *Magnetisation and Transition Metal Complexes*, eds. F. E. Mabbs and D. J. Machin, Chapman and Hall, London, 1973.
- 13 S. M. Gorun and S. J. Lippard, *Inorg. Chem.*, 1991, **30**, 1625.
- 14 J. Cosier and A. M. Glazier, *J. Appl. Crystallogr.*, 1986, **19**, 105.
- 15 W. Clegg, *Acta Crystallogr., Sect. A*, 1981, **37**, 22.
- 16 G. M. Sheldrick, SHELXS 86, program for crystal structure solution, *Acta Crystallogr., Sect. A*, 1990, **46**, 467.
- 17 G. M. Sheldrick, SHELXL 93, program for crystal structure refinement, University of Göttingen, 1993.
- 18 C. J. O'Connor, *Prog. Inorg. Chem.*, 1982, **29**, 203.
- 19 *Handbook of Chemistry and Physics*, ed. R. C. Weast, 70th edn., CRC Press, Boca Raton, FL, 1990, p. E134.
- 20 A. J. Blake, C. M. Grant, C. I. Gregory, S. Parsons, J. M. Rawson, D. Reed and R. E. P. Winpenny, *J. Chem. Soc., Dalton Trans.*, 1995, 163.
- 21 J. M. Rawson, University of Edinburgh, 1994.

Received 4th August 1995; Paper 5/05237H